Phys. – JETP 20, 997 (1965)].
[26]A. Lurio and R. Novick, Phys. Rev. 134, A608 (1964).
[27]H. A. Bethe and E. E. Salpeter, Quantum Mechanics of One- and Two-Electron Atoms (Springer-Verlag, Berlin, 1957).
[28]R. Lincke and H. R. Griem, Phys. Rev. 143,66 (1966).
[29]J. Geiger, Z. Physik 175, 530 (1963).

PHYSICAL REVIEW VOLUME 183, NUMBER 1 5 JULY 1969

Calculation of Bremsstrahlung Cross Sections with Sommerfeld-Maue Eigenfunctions

Gerhard Elwert and Eberhard Haug
Lehrstuhl für Theoretische Astrophysik der Universität Tübingen, Tübingen, Germany
(Received 11 December 1967; revised manuscript received 16 August 1968)

A formula for the differential cross section of bremsstrahlung is calculated with the aid of Sommerfeld-Maue eigenfunctions, i.e., under the assumption of a pure Coulomb field and low atomic numbers ($\alpha Z \ll 1$). This expression is valid for all energies of both electrons and photons, and it is shown that the previously well-known formulas of Sommerfeld, Sauter, Bethe, Heitler, Scherzer, and Bethe and Maximon are contained as special cases. Hence this cross section is correct for high electron energies and, apart from a small spin correction, for nonrelativistic energies even if $\alpha Z \ll 1$ is not satisfied. The formula has been programmed, and in addition total cross sections have been obtained by numerical integration over the angles of the emitted electrons and photons. Comparison with the Born approximation allows derivation of the Coulomb correction. Several cases of interest are compared with experiment, in particular the elementary bremsstrahlung process itself, for which experimental results are now available.

1. INTRODUCTION

The theory of bremsstrahlung has been the subject of a large number of papers in which various energy regions and different types of approximation for the interaction of the electrons with the atomic field have been considered. Whereas presently at any rate the interaction of electrons with the radiation field can be treated only by perturbation theory, their interaction with the field of the atomic nucleus can in principle be handled rigorously. In the latter case one uses as eigenfunctions for the electrons the exact Coulomb solutions for the nuclear electrostatic field, such that these solutions correspond asymptotically to plane waves and incoming or outgoing spherical waves.

Actually this treatment amounts to summing over-all (infinitely many) Feynman graphs representing the interaction of electrons with the nuclear field. In this way Sommerfeld[1] was the first to calculate the matrix element with Schrödinger eigenfunctions for the nonrelativistic case. For the relativistic energy domain it is also possible to use the same method at least in principle, but so far exact solutions for the Dirac equation including the Coulomb field with the above boundary conditions have only been found in series form as a summation over quantum number l.[2] Because of the large number of summands appearing in the matrix element, it would be extremely troublesome to perform these calculations numerically.

In fact, Sommerfeld and Maue[3] have already given a relativistic eigenfunction which is correct up to first order in αZ. Using the Sommerfeld-Maue eigenfunction, Elwert[4] first calculated the matrix element of the elementary process of the x-ray emission. His result was only reported[4] but not published in detail as the evaluation of the expression obtained was then (1938) too complicated to be performed. In the present paper we further develop the above expression for the differential cross section and apply it for various cases of interest. We obtain the formulas of Sommerfeld,[1] Sauter,[5] Bethe and Heitler,[6] and Scherzer[7] as special cases.

The theoretical differential cross section is compared with new coincidence experiments. The differential cross section has also been integrated numerically over the direction of the outgoing electrons and photons to obtain several comparisons between theory and experiment.

2. CALCULATION OF THE DIFFERENTIAL CROSS SECTION WITH SOMMERFELD-MAUE WAVE FUNCTIONS

According to the usual Feynman-Dyson formulation of quantum electrodynamics, for the processes in which an atomic field plays a role the interaction of the electrons with the radiation field as well as with the atomic field should be considered as perturbation. In the case of bremsstrahlung, the lowest-order graph corresponding to the first Born approximation is then of second order. If one incorporates, on the other hand, the interaction of the electrons with the atom in the unperturbed Hamiltonian, the lowest-order graph is of the first order only. This amounts to summing over infinitely many Feynman-Dyson graphs corresponding to the interaction of the electrons with the atomic field to any order, but with the radiation field to the first order only. This equivalence is shown in Fig. 1 in which the left graph represents the first-order matrix element calculated with the aid of the eigenfunctions of the Hamiltonian mentioned above. The double lines in Fig. 1 are used to denote electron propagation in the Coulomb field. This treatment corresponds to Furry's[8] extension of the Feynman-Dyson formalism by including the external potential in the field variables (Furry picture).

The Dirac equation for an electron in a Coulomb field of a nucleus with atomic number Z is

$$(i\vec{\alpha}\cdot\vec{\nabla}-\beta+\epsilon+a/r)\Psi=0, \tag{1}$$

where ϵ is the total energy of the electron in units of the rest energy mc^2, $a=\alpha Z$, $\alpha=e^2/\hbar c$ (Sommerfeld's fine structure constant), $\vec{\alpha}$ and β are the Dirac operators, and $\vec{r}$ the electron coordinate in the units of $\hbar/mc$. With this notation the Sommerfeld-Maue function has the form

$$\Psi_{SM}=Ne^{i\vec{p}\cdot\vec{r}}[1-(i/2\epsilon)\vec{\alpha}\cdot\vec{\nabla}]$$
$$\times F(ia\epsilon/p;1;ipr-i\vec{p}\cdot\vec{r})u(\vec{p}). \tag{2a}$$

Here $\vec{p}$ is the momentum of the electron in units of mc, N is a normalization factor, F is the confluent hypergeometric function with the indicated arguments, and $u(\vec{p})$ is the spinor of a free electron with momentum $\vec{p}$. Asymptotically for large r, Ψ_{SM} behaves like a plane wave plus an outgoing spherical wave. It agrees up to the first order in αZ with the exact solution of the Dirac equation. Comparing Ψ_{SM} with the exact Darwin eigenfunction, Bethe and Maximon[9] could show more precisely that all partial waves with $l^2 \gg \alpha^2Z^2$ are represented correctly.

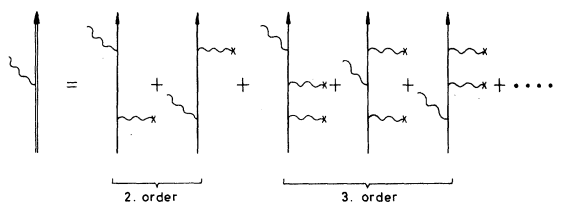

FIG. 1. Bremsstrahlung graph of the Furry picture and the equivalent sum of Feynman-Dyson graphs.

The matrix element for bremsstrahlung, incorporating the interaction with the radiation field to first order, is

$$M=C\int\Psi_2^{\dagger}(\vec{\alpha}\cdot\vec{e}^{*})e^{-i\vec{k}\cdot\vec{r}}\Psi_1 d\tau, \tag{3}$$

where $$C=-e\hbar c(2\pi/mc^2k)^{1/2}. \tag{4}$$

The subscript 1 refers to the incident electron, and the 2 to the final electron; $\vec{k}$ is the momentum of the outgoing photon in units of mc; and $\vec{e}$ its polarization vector; the photon energy is

$$k=\epsilon_1-\epsilon_2. \tag{5}$$

In our approximation Ψ_1 is given by the Sommerfeld-Maue function (2a). Ψ_2 has to behave asymptotically like a plane wave plus incoming spherical wave,[9,10] so we have

$$\Psi_2^{\dagger}=u^{\dagger}(\vec{p}_2)N_2^{*}e^{-i\vec{p}_2\cdot\vec{r}}[1+(i/2\epsilon_2)\vec{\alpha}\cdot\vec{\nabla}$$
$$\times F(ia\epsilon_2/p_2;1;ip_2r+i\vec{p}_2\cdot\vec{r}). \tag{2b}$$

Substitution of (2a) and (2b) in (3) gives

$$M=K[u^{\dagger}(\vec{p}_2)\vec{\alpha}\cdot\vec{e}^{*}u(\vec{p}_1)I_1$$
$$+u^{\dagger}(\vec{p}_2)(\vec{\alpha}\cdot\vec{e}^{*})(\vec{\alpha}\cdot\vec{I}_2)u(\vec{p}_1)$$
$$+u^{\dagger}(\vec{p}_2)(\vec{\alpha}\cdot\vec{I}_3)(\vec{\alpha}\cdot\vec{e}^{*})u(\vec{p}_1)$$
$$+u^{\dagger}(\vec{p}_2)I_4u(\vec{p}_1)], \tag{6}$$

where we used the following definitions:

$$K=(\hbar/mc)^3CN_1N_2^{*}, \tag{7}$$

$$a_1=a\epsilon_1/p_1,\quad a_2=a\epsilon_2/p_2, \tag{8}$$

$$I_1=\int e^{i\vec{q}\cdot\vec{r}}F(ia_2;1;ip_2r+i\vec{p}_2\cdot\vec{r})$$
$$\times F(ia_1;1;ip_1r-i\vec{p}_1\cdot\vec{r})d^3r, \tag{9}$$

$$\vec{I}_2=-\frac{i}{2\epsilon_1}\int e^{i\vec{q}\cdot\vec{r}}F(ia_2;1;ip_2r+i\vec{p}_2\cdot\vec{r})$$
$$\times[\vec{\nabla}F(ia_1;1;ip_1r-i\vec{p}_1\cdot\vec{r})]d^3r, \tag{10}$$

$$\vec{I}_3=\frac{i}{2\epsilon_2}\int e^{i\vec{q}\cdot\vec{r}}[\vec{\nabla}F(ia_2;1;ip_2r+i\vec{p}_2\cdot\vec{r})]$$
$$\times F(ia_1;1;ip_1r-i\vec{p}_1\cdot\vec{r})d^3r, \tag{11}$$

$$I_4=\frac{1}{4\epsilon_1\epsilon_2}\int e^{i\vec{q}\cdot\vec{r}}[\vec{\alpha}\cdot\vec{\nabla}F(ia_2;1;ip_2r+i\vec{p}_2\cdot\vec{r})]$$

$$\times\vec{\alpha}\cdot\vec{e}^{*}[\vec{\alpha}\cdot\vec{\nabla}F(ia_1;1;ip_1r-i\vec{p}_1\cdot\vec{r})]d^3r, \quad (12)$$

$$\vec{q}=\vec{p}_1-\vec{p}_2-\vec{k}. \quad (13)$$

The integral I_4 is proportional to $(\alpha Z)^2$. Besides the part of the matrix element containing I_4, other contributions of order $(\alpha Z)^2$ have to be considered for large Z, which result from higher-order terms of the correct wave functions. Since these integrals cannot be calculated generally, it is consistent to leave out the contribution due to I_4; that is, the resulting cross section holds for small atomic numbers Z. Bethe and Maximon[9] have, however, shown that I_4 and the other terms of higher order in αZ are negligible for energies large compared with the electron rest energy, and for small angles. Hence the cross section is valid for all Z in this case. In addition, Sommerfeld's formula for the nonrelativistic energy range can be derived from the cross section given in this paper (cf. Sec. 4). With a purely electrostatic potential the term due to spin-orbit coupling is of relative order $p\alpha Z$.[11] Thus the spin-effect correction to the nonrelativistic cross section is small for $p_1 \ll 1$ even if Z is large. Therefore for large nuclear charges the neglected terms of the matrix element are expected to be important only at intermediate energies. The integrals I_1, $\vec{I}_2$, and $\vec{I}_3$ have been evaluated by parametric differentiation of one scalar integral which can be computed exactly[4, 12]; one obtains

$$I_1=2K_1[\epsilon_2(A_1-B_1)-\epsilon_1(A_2+B_2)], \quad (14a)$$

$$\vec{I}_2=K_1[\vec{q}A_2+(\vec{P}/p_1+\vec{q})B_2], \quad (15a)$$

$$\vec{I}_3=K_1[\vec{q}A_1+(\vec{P}/p_2-\vec{q})B_1], \quad (16a)$$

where we used the notations

$$A_1=\frac{V-ia_1(1-x)W}{D_1q^2}, \quad A_2=\frac{V-ia_2(1-x)W}{D_2q^2}, \quad (17)$$

$$B_1=\frac{ia_1W}{D_1D_2}, \quad B_2=\frac{ia_2W}{D_1D_2}, \quad (18a)$$

$$D_1=2(\epsilon_1k-\vec{k}\cdot\vec{p}_1), \quad D_2=2(\epsilon_2k-\vec{k}\cdot\vec{p}_2), \quad (19)$$

$$\vec{P}=p_1\vec{p}_2+p_2\vec{p}_1, \quad (20)$$

and

$$K_1=4\pi a e^{-\pi a_1}(q^2/D_2)^{ia_1}(q^2/D_1)^{ia_2}. \quad (21)$$

V and W are the hypergeometric functions

$$V={}_2F_1(ia_1, ia_2; 1; x),$$
$$W={}_2F_1(1+ia_1, 1+ia_2; 2; x), \quad (22)$$

where $x=1-\mu q^2/D_1D_2$ (23)

and $\mu=(p_1+p_2)^2-k^2$. (24)

All the integrals considered [Eqs. (14a) to (16a)] are of the order αZ. Thus the corrections to the matrix element M and to the cross section, due to the neglected terms, are of relative order αZ.

After summing the absolute square of the matrix element M over the spins of the final electron and the polarization directions of the outgoing photon, and averaging over the spins of the incident electron, one obtains

$$\begin{aligned}\sum|M|^2=\frac{|K|^2}{\epsilon_1\epsilon_2}\Bigg\{&|I_1|^2\left(\epsilon_1\epsilon_2-1-\frac{\vec{k}\cdot\vec{p}_1\ \vec{k}\cdot\vec{p}_2}{k^2}\right)\\&+(|\vec{I}_2|^2+|\vec{I}_3|^2)\left(\epsilon_1\epsilon_2+1+\frac{\vec{k}\cdot\vec{p}_1\ \vec{k}\cdot\vec{p}_2}{k^2}\right)\\&-2\,\mathrm{Re}\left(\frac{\vec{I}_2^{*}\cdot\vec{k}\ \vec{I}_3\cdot\vec{k}}{k^2}\right)(\epsilon_1\epsilon_2+1+\vec{p}_1\cdot\vec{p}_2)\\&+2\,\mathrm{Re}\left[(\vec{I}_3^{*}-\vec{I}_2^{*})\cdot\left(\vec{p}_1\frac{\vec{I}_2\cdot\vec{k}\ \vec{p}_2\cdot\vec{k}}{k^2}-\vec{p}_2\frac{\vec{I}_3\cdot\vec{k}\ \vec{p}_1\cdot\vec{k}}{k^2}\right)\right]\\&+2\,\mathrm{Re}(\vec{I}_2^{*}\cdot\vec{p}_1\ \vec{I}_3\cdot\vec{p}_2-\vec{I}_3^{*}\cdot\vec{p}_1\ \vec{I}_2\cdot\vec{p}_2)\\&+2\epsilon_1\,\mathrm{Re}\left[I_1^{*}\left(\vec{I}_3\cdot\vec{p}_2-\frac{\vec{I}_2\cdot\vec{k}\ \vec{p}_2\cdot\vec{k}}{k^2}\right)\right]\\&+2\epsilon_2\,\mathrm{Re}\left[I_1^{*}\left(\vec{I}_2\cdot\vec{p}_1-\frac{\vec{I}_3\cdot\vec{k}\ \vec{p}_1\cdot\vec{k}}{k^2}\right)\right]\\&+2\,\mathrm{Re}\vec{I}_2^{*}\cdot\vec{I}_3\left(\vec{p}_1\cdot\vec{p}_2-\frac{\vec{k}\cdot\vec{p}_1\ \vec{k}\cdot\vec{p}_2}{k^2}\right)\Bigg]\Bigg\}. \quad (25)\end{aligned}$$

This formula has been derived by Elwert[4] in 1938. The cross section is given by

$$d\sigma=(2\pi/\hbar)(\epsilon_1/p_1c)d\rho_f\sum|M|^2, \quad (26)$$

in which the density of the final states is

$$d\rho_f=\frac{(mc^2)^5}{(2\pi\hbar c)^6}p_2\epsilon_2d\Omega p_2k^2d\Omega_k dk. \quad (27)$$

$d\Omega_{p_2}$ and $d\Omega_k$ are infinitesimal solid angles around the vectors $\vec{p}_2$ and $\vec{k}$.

Normalizing the asymptotic expressions for ψ_1 and ψ_2 to unit amplitude, we have

$$|N_1|^2=2\pi a_1/(1-e^{-2\pi a_1}) \quad (28)$$

and $$|N_2|^2=2\pi a_2/(1-e^{-2\pi a_2}). \quad (29)$$

Substituting Eqs. (4), (7), (14a), (15a), (16a), (21), (25), and (27)–(29) in (26), we obtain for the differential cross section of bremsstrahlung

$$\begin{aligned}d^3\sigma=&\frac{2\pi a_1}{e^{2\pi a_1}-1}\frac{2\pi a_2}{1-e^{-2\pi a_2}}\frac{r_0^2}{\pi^2}\alpha Z^2\frac{p_2}{p_1}\\&\times k\,dk\,d\Omega_k\,d\Omega_{p_2}[E_1|A_1|^2+E_2|A_2|^2\\&-2E_3\,\mathrm{Re}(A_1^{*}A_2)-2F_1\,\mathrm{Re}(A_1^{*}B)\end{aligned}$$

$$- 2F_2 \mathrm{Re}(A_2^* B) + F_3 |B|^2]. \tag{30}$$

In this formula the classical electron radius $r_0 = e^2/mc^2$, and the following definitions are used:

$$B = iaW/D_1 D_2 , \tag{18b}$$

$$E_1 = (4\epsilon_2^2 - q^2)\eta_1^2 + \left(\frac{2k^2}{D_2}(\eta_2^2 + 1) + \eta_1^2 - \vec{\eta}_1 \cdot \vec{\eta}_2\right) D_1 , \tag{31}$$

$$\begin{aligned}
E_2 &= (4\epsilon_1^2 - q^2)\eta_2^2 + \left(\frac{2k^2}{D_1}(\eta_1^2 + 1) - \eta_2^2 + \vec{\eta}_1 \cdot \vec{\eta}_2\right) D_2 , \\
E_3 &= (4\epsilon_1\epsilon_2 - q^2)\vec{\eta}_1 \cdot \vec{\eta}_2 + \tfrac{1}{2} D_1 (\vec{\eta}_1 \cdot \vec{\eta}_2 - \eta_2^2) \\
&\quad + \tfrac{1}{2} D_2 (\eta_1^2 - \vec{\eta}_1 \cdot \vec{\eta}_2) + 2k^2 (\vec{\eta}_1 \cdot \vec{\eta}_2 + 1); \\
F_1 &= k\rho(\eta_1^2 - \vec{\eta}_1 \cdot \vec{\eta}_2) \\
&\quad + \kappa[\vec{k} \cdot \vec{p}_1 (\vec{p}_1 \cdot \vec{p}_2 - \vec{k} \cdot \vec{p}_2 + p_2^2) + 2k^2] \\
&\quad - (\kappa p_1 p_2 - 2k/p_1)(\vec{k} \cdot \vec{p}_1 + \vec{k} \cdot \vec{p}_2 - k^2) , \\
F_2 &= k\rho(\eta_2^2 - \vec{\eta}_1 \cdot \vec{\eta}_2) \\
&\quad + \kappa[\vec{k} \cdot \vec{p}_2 (\vec{p}_1 \cdot \vec{p}_2 + \vec{k} \cdot \vec{p}_1 + p_1^2) - 2k^2] \\
&\quad - (\kappa p_1 p_2 + 2k/p_2)(\vec{k} \cdot \vec{p}_1 + \vec{k} \cdot \vec{p}_2 + k^2) , \\
F_3 &= \mu\left(k^2 - \frac{\vec{k} \cdot \vec{p}_1 \ \vec{k} \cdot \vec{p}_2}{p_1 p_2} + \frac{p_1^2 - p_2^2}{p_1^2 p_2^2}\right. \\
&\quad \left. \times (p_1^2 - p_2^2 + \vec{k} \cdot \vec{p}_1 + \vec{k} \cdot \vec{p}_2)\right) - 2k^2\rho^2 ;
\end{aligned} \tag{32}$$

$$\vec{\eta}_1 = \vec{p}_1 \times \vec{k}/k , \quad \vec{\eta}_2 = \vec{p}_2 \times \vec{k}/k ,$$

$$\begin{aligned}
\vec{\eta}_1 \cdot \vec{\eta}_2 &= (\vec{p}_1 \times \vec{k}) \cdot (\vec{p}_2 \times \vec{k})/k^2 \\
&= \vec{p}_1 \cdot \vec{p}_2 - \vec{k} \cdot \vec{p}_1 \ \vec{k} \cdot \vec{p}_2/k^2 ;
\end{aligned} \tag{33}$$

$$\kappa = \epsilon_1/p_1 + \epsilon_2/p_2 , \quad \rho = 1/p_1 + 1/p_2 .$$

$d^3\sigma$ is the probability that an electron of energy ϵ_1 is scattered in the direction of $\vec{p}_2$, and at the same time a photon is emitted in the direction of $\vec{k}$ with the energy $k = \epsilon_1 - \epsilon_2$ (elementary process of bremsstrahlung production).

The above formula for $d^3\sigma$ imitates Sommerfeld's nonrelativistic cross section which also contains the quantities A_1 and A_2. So the transition to the nonrelativistic limit can be achieved in a particularly simple way. The other possible ways of writing the expression (30) using different parameters are more extensive.

If we choose a coordinate system such that its z axis has the direction of $\vec{k}$ then the vectors $\vec{p}_1$ and $\vec{p}_2$ can be represented by

$$\begin{aligned}
\vec{p}_1 &= p_1\{\sin\theta_1 \cos\phi_1, \ \sin\theta_1 \sin\phi_1, \ \cos\theta_1\} , \\
\vec{p}_2 &= p_2\{\sin\theta_2 \cos\phi_2, \ \sin\theta_2 \sin\phi_2, \ \cos\theta_2\} , \\
\vec{k} &= k\{0, 0, 1\} ,
\end{aligned} \tag{34}$$

and the scalar and vector products by

$$\begin{aligned}
\vec{p}_1 \cdot \vec{p}_2 &= p_1 p_2 \\
&\quad \times [\cos\theta_1 \cos\theta_2 + \sin\theta_1 \sin\theta_2 \cos(\phi_1 - \phi_2)] , \\
\vec{k} \cdot \vec{p}_1 &= kp_1 \cos\theta_1 , \quad \vec{k} \cdot \vec{p}_2 = kp_2 \cos\theta_2 , \\
(\vec{p}_1 \times \vec{k})^2 &= k^2 p_1^2 \sin^2\theta_1 , \\
(\vec{p}_2 \times \vec{k})^2 &= k^2 p_2^2 \sin^2\theta_2 ,
\end{aligned} \tag{35}$$

and the elements of solid angle by

$$d\Omega_k = \sin\theta_1 \, d\theta_1 d\phi_1 , \quad d\Omega_{p_2} = \sin\theta_2 \, d\theta_2 d\phi_2 . \tag{36}$$

Because $d^3\sigma$ depends only on the difference $\phi = \phi_1 - \phi_2$ of the azimuthal angles, the later integration over ϕ_1 gives simply a factor 2π.

3. BETHE-HEITLER-SAUTER FORMULA (FIRST BORN APPROXIMATION)

In the case of low atomic numbers Z and sufficiently high energies ϵ_1 and ϵ_2, that is, for $a_1 \ll 1, a_2 \ll 1$, we can approximate $V \simeq 1$, $aW \simeq 0$, and put

$$[2\pi a_1/(e^{2\pi a_1} - 1)][2\pi a_2/(1 - e^{-2\pi a_2})]$$

approximately equal to one. Then we obtain

$$A_1 \simeq 1/D_1 q^2 , \quad A_2 \simeq 1/D_2 q^2 , \quad B \simeq 0 , \tag{37}$$

and the cross section is

$$\begin{aligned}
d^3\sigma_B &= (r_0^2/\pi^2)\alpha Z^2 (p_2/p_1) q^{-4} k dk d\Omega_k d\Omega_{p_2} [(\eta_1^2/D_1^2)(4\epsilon_2^2 - q^2) \\
&\quad + (\eta_2^2/D_2^2)(4\epsilon_1^2 - q^2) - 2(\vec{\eta}_1 \cdot \vec{\eta}_2/D_1 D_2)(4\epsilon_1\epsilon_2 - q^2) + (2k^2/D_1 D_2)(\vec{\eta}_1 - \vec{\eta}_2)^2] .
\end{aligned} \tag{38}$$

This is the bremsstrahlung cross section as calculated by Sauter[5] and Bethe and Heitler[6] using the first Born approximation. If one introduces the coordinate system of Eq. (34), one obtains an expression which can be integrated over the solid angles $d\Omega_{p_2}$ and $d\Omega_k$ in closed form. If the electrons are of high energies and $|\vec{q}|$ is not near its minimum value, the expression (38) is in good agreement with (30).[9] In the short-wavelength limit ($\epsilon_2 = 1, p_2 = 0$) contrary to Eq. (30), the expression (38) gives zero intensity.

4. NONRELATIVISTIC APPROXIMATION

The differential cross section for bremsstrahlung in the case of nonrelativistic energies can be obtained from Eq. (30) by taking the following limits:

$$\epsilon_{1,2} \to 1, \quad p_{1,2} \to \beta_{1,2} \ll 1, \quad k \to \tfrac{1}{2}(\beta_1^2 - \beta_2^2), \quad \mu \to (\beta_1 + \beta_2)^2 . \tag{39}$$

Here β_1 and β_2 are the electron velocities in the initial and final state respectively in units of the velocity of light. Neglecting terms of the order β^2 compared with unity, we obtain from Eqs. (30) to (33)

$$d^3\sigma_{\mathrm{NR}} = \frac{2\pi a/\beta_1}{e^{2\pi a/\beta_1} - 1} \frac{2\pi a/\beta_2}{1 - e^{-2\pi a/\beta_2}} \frac{r_0^2}{\pi^2} \alpha Z^2 \frac{\beta_2}{\beta_1} \frac{dk}{k} d\Omega_k d\Omega_{p_2} \frac{1}{q^4}$$

$$\times \left| \frac{\beta_1}{S_1} \frac{\vec{p}_1 \times \vec{k}}{p_1 k} \left(V - i \frac{a}{\beta_1} (1-x) W \right) - \frac{\beta_2}{S_2} \frac{\vec{p}_2 \times \vec{k}}{p_2 k} \left(V - i \frac{a}{\beta_2} (1-x) W \right) \right|^2 , \tag{40}$$

where

$$S_1 = 1 - \vec{k} \cdot \vec{p}_1/k = 1 - \beta_1 \cos\theta_1, \quad S_2 = 1 - \vec{k} \cdot \vec{p}_2/k = 1 - \beta_2 \cos\theta_2 \tag{41}$$

and

$$V = {}_2F_1\left(\frac{ia}{\beta_1}, \frac{ia}{\beta_2}; 1; x\right), \quad W = {}_2F_1\left(\frac{ia}{\beta_1} + 1, \frac{ia}{\beta_2} + 1; 2; x\right), \quad x = 1 - \frac{q^2}{(\beta_1 - \beta_2)^2 S_1 S_2} . \tag{42}$$

Equation (40) agrees with the cross section for bremsstrahlung of nonrelativistic electrons which has been calculated with Schrödinger eigenfunctions taking retardation into account.[4] Neglecting, in addition, terms of the order β compared with 1, one gets $S_1 \simeq S_2 \simeq 1$ and obtains

$$d^3\sigma_{\mathrm{NR}} = \frac{2\pi a/\beta_1}{e^{2\pi a/\beta_1} - 1} \frac{2\pi a/\beta_2}{1 - e^{-2\pi a/\beta_2}} \frac{r_0^2}{\pi^2} \alpha Z^2 \frac{\beta_2}{\beta_1} \frac{dk}{k} d\Omega_k d\Omega_{p_2} \frac{1}{q^4}$$

$$\times \left| \beta_1 \frac{\vec{p}_1 \times \vec{k}}{p_1 k} \left(V - i \frac{a}{\beta_1} (1-x) W \right) - \beta_2 \frac{\vec{p}_2 \times \vec{k}}{p_2 k} \left(V - i \frac{a}{\beta_2} (1-x) W \right) \right|^2 . \tag{43}$$

This equation corresponds to Sommerfeld's method of matrix elements $\vec{M} = \int \psi_2^* \vec{r} \psi_1 d\tau$ in the earlier nonrelativistic calculation without retardation.[1]

5. THE SHORT-WAVELENGTH LIMIT

In the short-wavelength limit of bremsstrahlung, the photon receives the total kinetic energy E_1 of the incident electron, and the momentum $\vec{p}_2$ of the outgoing electron is zero. Then it follows that

$$k \to \epsilon_1 - 1, \quad q^2 \to D_1, \quad D_2 \to 2k, \quad \mu \to 2k . \tag{44}$$

Further $a_2 = a\epsilon_2/p_2$ goes to infinity and $x = 1 - \mu q^2/D_1 D_2$ will be zero; because $a_2 x$ remains finite, the hypergeometric functions V and W become the confluent hypergeometric functions V_0 and W_0

$$V = {}_2F_1(ia_1, ia_2; 1; x) \to V_0 = F(ia_1; 1; i\xi), \tag{45a}$$

$$W = {}_2F_1(1 + ia_1, 1 + ia_2; 2; x) \to W_0 = F(1 + ia_1; 2; i\xi), \tag{45b}$$

where

$$\xi = \lim_{p_2 \to 0} a_2 x = a\left(2 \frac{\vec{q} \cdot \vec{p}_2}{q^2 p_2} - \frac{\vec{k} \cdot \vec{p}_2}{k p_2} - \frac{p_1}{k} \right). \tag{46}$$

One notes that the cross section depends on the direction of the outgoing electron, although it has zero velocity. Since some of the quantities in Eqs. (32) and (33) tend to infinity, we expediently do not use formula (30) to perform the limit $p_2 \to 0$ but go back to Eqs. (14a) to (29). From (14a) to (16a) we get

$$I_{10} = \lim_{p_2 \to 0} I_1 = \frac{K_1}{q^2}\left[\left(\frac{2}{q^2} - \frac{\epsilon_1}{k}\right)(V_0 - ia_1 W_0) + \epsilon_1 \frac{\vec{k}\cdot\vec{p}_2}{k^2 p_2} ia W_0\right], \tag{14b}$$

$$\vec{I}_{20} = \lim_{p_2 \to 0} \vec{I}_2 = \frac{K_1}{2kq^2}\left[\vec{q}(V_0 - ia_1 W_0) + \left(\frac{\vec{k}}{p_1} + \frac{\vec{p}_2}{p_2} - \frac{\vec{k}\cdot\vec{p}_2}{kp_2}\vec{q}\right) ia W_0\right], \tag{15b}$$

and

$$\vec{I}_{30} = \lim_{p_2 \to 0} \vec{I}_3 = \frac{K_1}{q^2}\left[\frac{\vec{q}}{q^2}(V_0 - ia_1 W_0) + \frac{\epsilon_1}{2k}\left(\frac{\vec{k}}{p_1} + \frac{\vec{p}_2}{p_2}\right) ia W_0\right]. \tag{16b}$$

Substituting these expressions in (25), we obtain for the differential cross section at the short-wavelength limit

$$\begin{aligned} d^3\sigma_0 = {} & \frac{2\pi a_1}{e^{2\pi a_1} - 1} \frac{r_0^2}{\pi} \alpha^2 Z^3 \frac{1}{k p_1 q^4} dk d\Omega_k d\Omega_{p_2} \Bigg\{ 2\left(\frac{4}{q^2} + k - 1\right) \frac{(\vec{p}_1 \times \vec{k})^2}{q^2} |V_0 - ia_1 W_0|^2 \\ & + \left[\left(1 - 2\frac{\epsilon_1^2 + \epsilon_1 + 2}{q^2}\right) \frac{(\vec{p}_1 \times \vec{k})\cdot(\vec{p}_2 \times \vec{k})}{kp_2} - 2\left(\frac{k^2}{p_1} + \frac{\vec{k}\cdot\vec{p}_2}{kp_2}\right) \frac{(\vec{p}_1 \times \vec{k})^2}{q^2} + \left(1 - \frac{2k}{q^2}\right) \frac{\vec{k}\cdot\vec{p}_1\, \vec{k}\cdot\vec{p}_2}{p_2} \right. \\ & \left. + \left(1 + \frac{2k}{q^2}\right) \frac{k^2}{p_2} \vec{k}\cdot\vec{p}_2 \right] a\left[a_1 |W_0|^2 - \mathrm{Im}(V_0 W_0^*)\right] \\ & + \left[(2\epsilon_1^2 - k)\left(\frac{\vec{p}_2 \times \vec{k}}{p_2 k}\right)^2 + \frac{\vec{k}\cdot\vec{p}_2}{k^2 p_2^2}(\vec{p}_1 \times \vec{k})\cdot(\vec{p}_2 \times \vec{k}) - k\frac{\vec{k}\cdot\vec{p}_1\ \vec{k}\cdot\vec{p}_2}{p_1 p_2} + k^3\right] a^2 |W_0|^2 \Bigg\}. \end{aligned} \tag{47}$$

Putting $a_1 \ll 1$ and neglecting terms of order a_1^2 in the bracket of $d^3\sigma_0$, one obtains

$$d^3\sigma_0 \approx \frac{2r_0^2}{\pi} \alpha^2 Z^3 \frac{2\pi a_1}{e^{2\pi a_1} - 1} \frac{(\vec{p}_1 \times \vec{k})^2}{k p_1 q^6}\left(\frac{4}{q^2} + k - 1\right) dk d\Omega_k d\Omega_{p_2}. \tag{48}$$

This formula can be derived from the expression given by Scherzer[7] for the radiation intensity at the short-wavelength limit if one sums over the two directions of polarization.

6. APPROXIMATION FOR THE LONG-WAVELENGTH LIMIT AND FOR HIGH ELECTRON ENERGIES

The argument x of the hypergeometric functions V and W is never positive. It is equal to zero at the short-wavelength limit as well as for

$$\phi = 0, \quad \sin\theta_2 = \sin\theta_1 \frac{\epsilon_2(\epsilon_1 - p_1\cos\theta_1) - p_2(\epsilon_1\cos\theta_1 - p_1)}{(\epsilon_1 - p_1\cos\theta_1)^2 + p_2^2 \sin^2\theta_1}. \tag{49}$$

$|x|$ is large as compared with unity on the following conditions:

(a) At the long-wavelength limit ($p_2 \simeq p_1$, $k \ll p_2$) except $q \simeq q_{\min} = p_1 - p_2 - k$.

(b) At high electron energies ($\epsilon_1 \gg 1$, $\epsilon_2 \gg 1$) except $q \simeq q_{\min}$.

In both cases we have $a_2 \simeq a_1$. The case (b) was investigated by Bethe and Maximon.[9] Now we suppose $|x| \gg 1$ in general. It is then convenient to make use of the following transformation for the hypergeometric functions:

$$\begin{aligned} V = {}_2F_1(ia_1, ia_2; 1; x) = {} & \frac{iG}{a_1}(1-x)^{-ia_1}\, {}_2F_1\left(ia_1, 1 - ia_2; 1 - ia_2 + ia_1; \frac{1}{1-x}\right) \\ & + \frac{iG^*}{a_2}(1-x)^{-ia_2}\, {}_2F_1\left(ia_2, 1 - ia_1; 1 + ia_2 - ia_1; \frac{1}{1-x}\right), \end{aligned} \tag{50}$$

$$\begin{aligned} W = {}_2F_1(1 + ia_1, 1 + ia_2; 2; x) = {} & \frac{G}{a_1 a_2 (1-x)}(1-x)^{-ia_1}\, {}_2F_1\left(1 + ia_1, 1 - ia_2; 1 - ia_2 + ia_1; \frac{1}{1-x}\right) \\ & + \frac{G^*}{a_1 a_2 (1-x)}(1-x)^{-ia_2}\, {}_2F_1\left(1 + ia_2, 1 - ia_1; 1 + ia_2 - ia_1; \frac{1}{1-x}\right), \end{aligned} \tag{51}$$

where $G=\Gamma(ia_2-ia_1)/\Gamma(ia_2)\Gamma(-ia_1)$. (52)

Expanding the hypergeometric functions ${}_2F_1$ to the order $(1-x)^{-1}$, performing the limit $a_2\to a_1$ and using the well-known properties of the Γ function, one obtains

$$\lim_{a_2\to a_1}|V-ia_1(1-x)W|^2\approx\left(\frac{\sinh(\pi a_1)}{\pi a_1}\right)^2\left(1-\frac{2a_1^2}{1-x}[\ln(1-x)+1-2\gamma-2\mathrm{Re}\psi(ia_1)]\right), \tag{53}$$

$$\lim_{a_2\to a_1}|W|^2\approx\left(\frac{\sinh(\pi a_1)}{\pi a_1}\right)^2\left(\frac{\ln(1-x)-2\gamma-2\mathrm{Re}\psi(ia_1)}{1-x}\right)^2\left(1+2\frac{1+a_1^2}{1-x}\right), \tag{54}$$

and

$$\lim_{a_2\to a_1}\{(1-x)a_1|W|^2-\mathrm{Im}(VW^*)\}\approx a_1\left(\frac{\sinh(\pi a_1)}{\pi a_1}\right)^2\frac{\ln(1-x)-2\gamma-2\mathrm{Re}\psi(ia_1)}{(1-x)^2}[\ln(1-x)-2\gamma-2\mathrm{Re}\psi(ia_1)-4a_1^2], \tag{55}$$

where

$$\psi(ia_1)=\frac{\Gamma'(ia_1)}{\Gamma(ia_1)},\quad \gamma=\lim_{m\to\infty}\left(1+\frac{1}{2}+\frac{1}{3}+\cdots+\frac{1}{m}-\ln m\right)\approx 0.577,\quad \gamma+\mathrm{Re}\psi(ia_1)=a_1^2\sum_{m=1}^{\infty}\frac{1}{m(m^2+a_1^2)}. \tag{56}$$

It is seen from Eqs. (54) and (55) that the terms of the bremsstrahlung cross section (30) proportional to $\mathrm{Re}(A_1^*B)$, $\mathrm{Re}(A_2^*B)$, and $|B|^2$ are of the order $[\ln(1-x)/(1-x)]^2$, so that we obtain up to order $\ln(1-x)/(1-x)$,

$$\begin{aligned} d^3\sigma &\simeq d^3\sigma_B[\pi a_1/\sinh(\pi a_1)]^2\,|V-ia_1(1-x)W|^2 \\ &\simeq d^3\sigma_B\{1-[2a_1^2/(1-x)]\,[\ln(1-x)+1-2\gamma-2\mathrm{Re}\psi(ia_1)]\}. \end{aligned} \tag{57}$$

That is, for $1-x\gg 1$ and $(a_2-a_1)/a_2\ll 1$, the bremsstrahlung differential cross section in Born approximation $d^3\sigma_B$ is correct. This is an extension of an earlier result[4] showing that the Born-approximation cross section is valid at the long-wavelength limit for nonrelativistic energies. In case (b), i.e., if one sets $a_1\simeq a_2\simeq a$, the correction factor to $d^3\sigma_B$ in Eq. (57) is the same as in the work of Bethe and Maximon[9] (note the different definitions of V, W, and x). Formula (57) will be used to evaluate the screening correction to the bremsstrahlung cross section near the long-wavelength limit (cf. Sec. 9).

7. PHOTON AND ELECTRON DISTRIBUTIONS

The general formula (30) for the differential cross section has been programmed for a Siemens 2002 computer. The differential cross section $d^3\sigma$ was determined for the case when the electrons and photons are emitted into the same plane. Then $\phi=\phi_1-\phi_2=0$. It is expedient to introduce the angles θ_1 and $\theta_e=\theta_1-\theta_2$, giving, with respect to the direction of the incoming electron, the directions of the emitted photon and the outgoing electron, respectively. Figure 2 shows isolines of the differential cross section in the $\theta_1-\theta_e$ plane for $Z=13$ and kinetic energies $E_1=180$ keV and $E_2=90$ keV. The diagram represents the angular correlations of both particles. One sees that the electrons and photons are predominantly emitted in the same direction. Examples of photon and electron distributions are drawn in Figs. 3 to 11. They correspond to the intersections (profiles) of relief maps as drawn in Fig. 2 by planes parallel to θ_1 or θ_e axis. The photon distributions have the scattering angle θ_e as parameter, and the electron distributions have the angle θ_1 as parameter. The curves show patterns directed strongly in the forward direction. For comparison with experiments in some of the following figures, Eq. (30) was applied as well, in order to calculate cross sections for $Z=79$, although the condition $\alpha Z\ll 1$ is violated. In Figs. 3 and 4, the photon distributions for $E_1=300$ keV, $E_2=170$ keV, $\theta_e=0°$, and $\theta_e=5°$ are given. Additionally the results of Born's approximation are drawn for comparison. The position of the maxima of the distribution curves is very little influenced, but the absolute values of the cross section do change. In the main lobe, these differences decrease with increasing θ_e. Recently Nakel[13,14] performed coincidence experiments to observe the elementary process of bremsstrahlung with thin targets for the same parameters as used in Figs. 3 and 4. These measurements are represented in Figs. 5 and 6. Figure 7 shows an electron distribution in the neighborhood of the long-wavelength limit and its com-

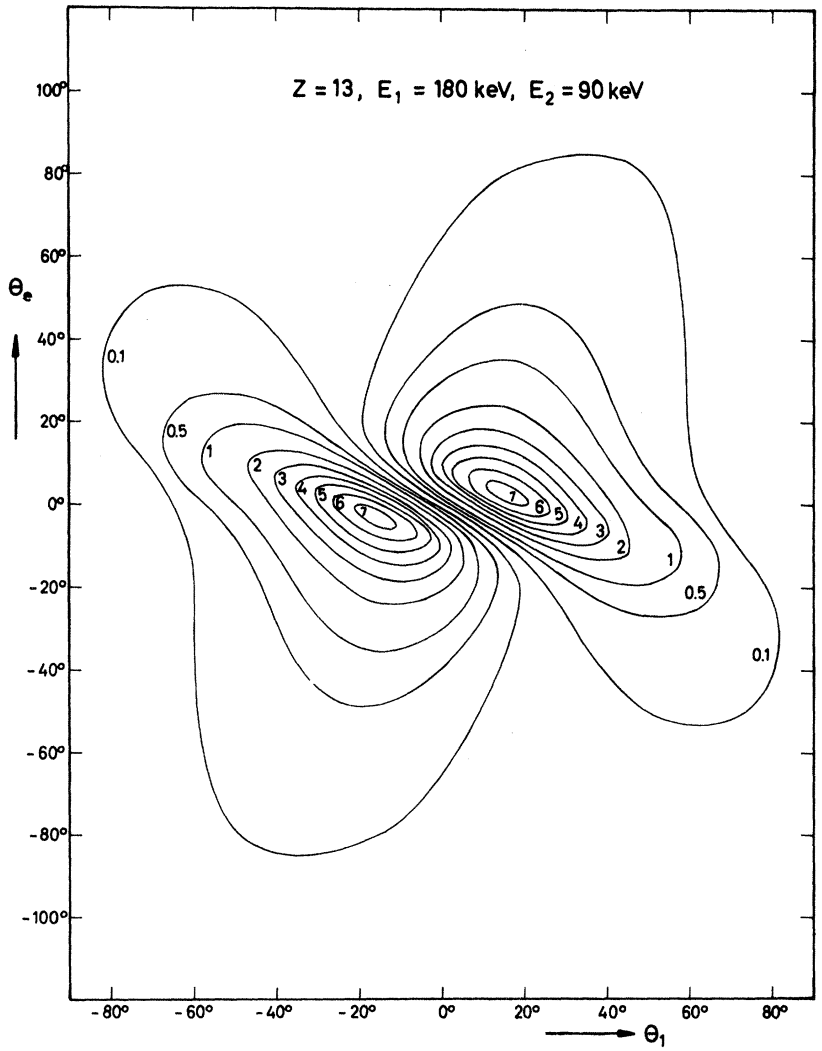

FIG. 2. Isolines of the differential cross section.

parison with a measurement of Hub and Nakel.[15] The theoretical cross sections given in Figs. 5 to 7 have been corrected for the finite angular resolution. As the experimental values are only relative, they have been adjusted at the maximum of $d^3\sigma$. The remaining "filling up" of the minima in the experimental photon distributions is probably due to the thickness of the target. Nevertheless the agreement between measurement and theory is good. Figure 8 shows the increase of asymmetry in the photon distributions and the vanishing of the minimum between the two lobes with increasing θ_e. The corresponding electron distributions for fixed angle θ_1 are given in Fig. 9. Figure 10 shows that the photon distributions at the short-wavelength limit become broader, and the minima are "filled up" more. The maximum values of $d^3\sigma$ are now attained at larger angles θ_1 and θ_e. The electron distributions at the short-wavelength limit are very broad and the maxima are even directed backwards. Details may be seen in the work of Haug.[16] With increasing electron energies, the photon distributions become narrower. An example is given in Fig. 11.

8. INTEGRATED CROSS SECTION $d^2\sigma$

For the cross section $d^2\sigma$ integrated over all directions of outgoing electrons

$$\frac{d^2\sigma}{dkd\Omega_k} = \int \frac{d^3\sigma}{dkd\Omega_k d\Omega_{p_2}} d\Omega_{p_2}, \tag{58}$$

more possibilities for comparison with experiment exist. Because the hypergeometric functions V and W occur in Eq. (30) for $d^3\sigma$, the integral can be computed numerically only. In Fig. 12 the integrated photon distributions have been plotted for $Z = 8$ (O) and $Z = 13$ (Al), $E_1 = 45$ keV and $h\nu = 40$ keV. These curves agree fairly well with the experimental data of Roess[17] who used a target of Al_2O_3. If we exclude angles smaller than 30° in forward direction $\theta_1 = 0°$ and angles

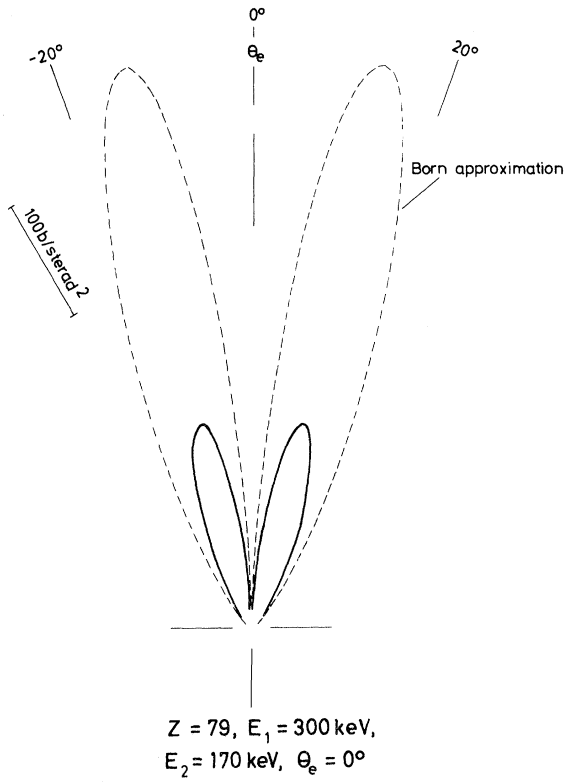

FIG. 3. Theoretical photon distributions for the electron angle $\theta_e = 0^0$.

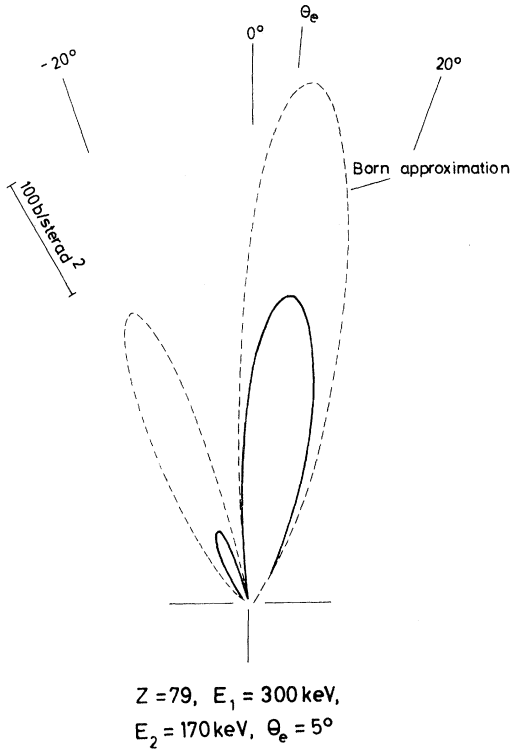

FIG. 4. Theoretical photon distributions for the electron angle $\theta_e = 5^0$.

$\theta_1 > 120°$, his points lie between the computed curves for both elements. However, the results of the calculations with the Born approximation are far off, which is to be expected at these low energies. It is to be noted that also the nonrelativistic approximation, Eq. (40), is very bad; the electron velocity at 45 keV is indeed relativistic. In this and the following figures the cross section has been multiplied by k for scaling reasons and divided by Z^2 to dispose of the main Z dependence. In the Born approximation $d^3\sigma/Z^2$ is independent of Z [see Eq. (38)]. An example of these cross sections as a function of the photon energy $h\nu$ is given in Fig. 13 for the angle $\theta_1 = 55°$. These should again be compared with the experimental points of Roess.[17] Additional curves for different values of θ_1 are given by Haug.[16]

At $E_1 = 180$ keV and $Z = 13$ there is very good agreement between the computed cross sections and experimental data of Klasmeier[18] on Al_2O_3, especially for large angles (Fig. 14). This agreement, however, gets worse if one goes to high atomic numbers (Fig. 15).

A comparison of our theory with measurements of Motz[19] at energies of the order of magnitude of the electron rest energy mc^2 shows noticeable

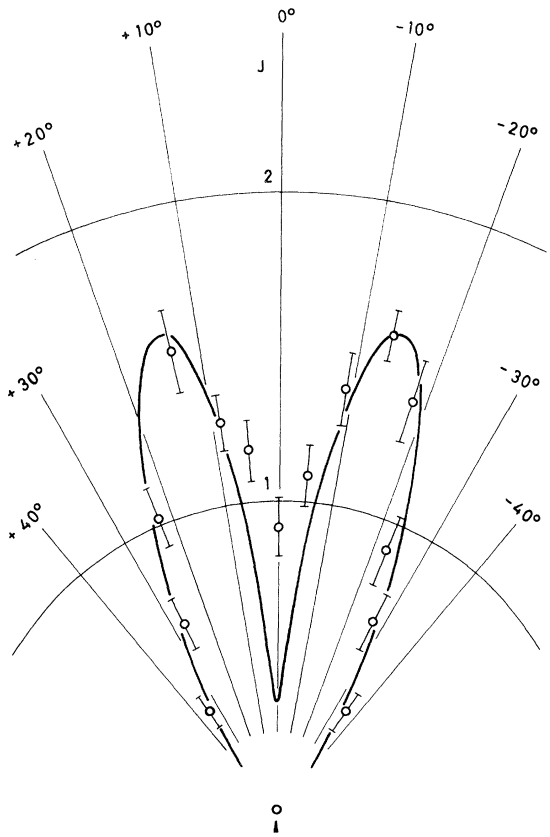

FIG. 5. Comparison between theoretical and observed photon distributions for the electron angle $\theta_e = 0^0$.

discrepancies. Most of the experimental cross sections are considerably larger than the computed ones.[16] Yet recent measurements of Rester and Dance[20] yield results which are lower than those of Motz by a factor up to 2. At energies large as compared with mc^2, the agreement with experiments of Starfelt and Koch[21] is good even for high atomic numbers (Fig. 16). This is to be expected, as for high energies the important values of the orbital angular momentum l are much larger than 1, so that for these l the condition $a^2 \ll l^2$ (see Ref. 9) is fulfilled for $a \approx 1$ too.

9. SCREENING CORRECTION

In Sec. 6 we have shown that the Born-approximation cross section $d^3\sigma_B$ is correct at the long-wavelength limit, hence the screening of the nucleus by the electron shell can be taken into account by multiplying $d^3\sigma_B$ by

$$F_S = [1 - F(\vec{q}, Z)]^2, \tag{59}$$

where $F(\vec{q}, Z)$ is the atomic form factor. An exception is the region in which q is close to its minimum value $q_{\min}$. In this case, however, the cross section is considerably reduced by the factor F_S, since we have complete screening near the long-wavelength limit. Thus the Born approximation can be used to calculate the screening correction to the integrated cross section in the neighborhood of the long-wavelength limit of bremsstrahlung. This was done for the curves in Figs. 13 to 16. The results have been extrapolated towards the short-wavelength limit. Figures 14 and 16 show that the screening correction increases the parallel run of the experimental and theoretical curves. In these calculations the Molière approximation[22] of the Thomas-Fermi model was used, where

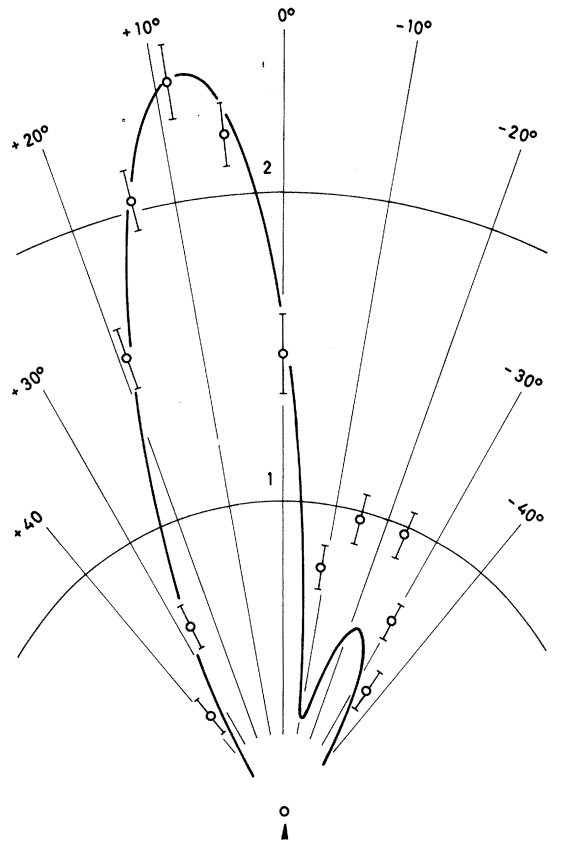

FIG. 6. Comparison between theoretical and observed photon distributions for the electron angle $\theta_e = 5^0$.

$$1 - F(\vec{q}, Z) = \sum_{i=1}^{3} \frac{\alpha_i q^2}{q^2 + \beta_i^2}; \quad \beta_i = \frac{b_i}{121} Z^{1/3}, \tag{60}$$

with

$$\alpha_1 = 0.1, \quad \alpha_2 = 0.55, \quad \alpha_3 = 0.35;$$
$$b_1 = 6, \quad b_2 = 1.2, \quad b_3 = 0.3. \tag{61}$$

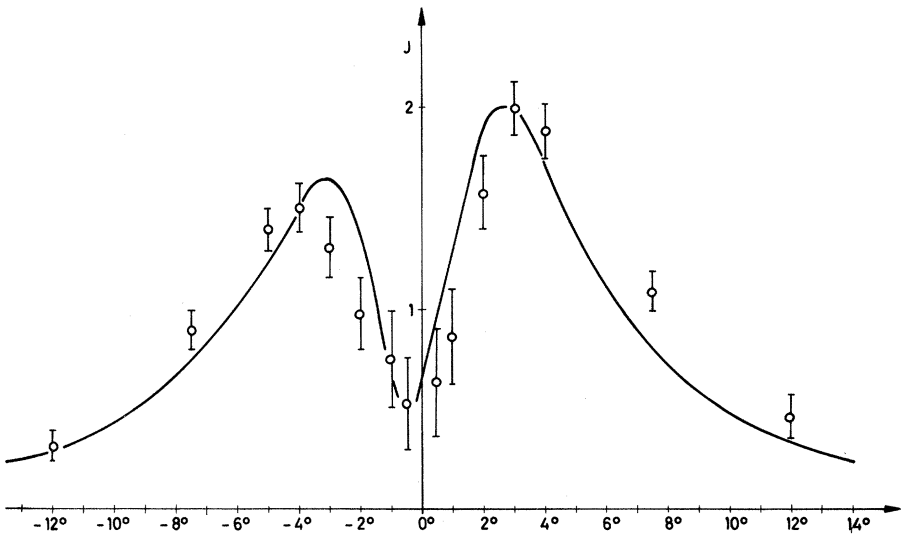

FIG. 7. Comparison between theoretical and observed electron distributions for $Z = 13$, $E_1 = 300$ keV, $E_2 = 225$ keV, and the photon angle $\theta_1 = 2^0$.

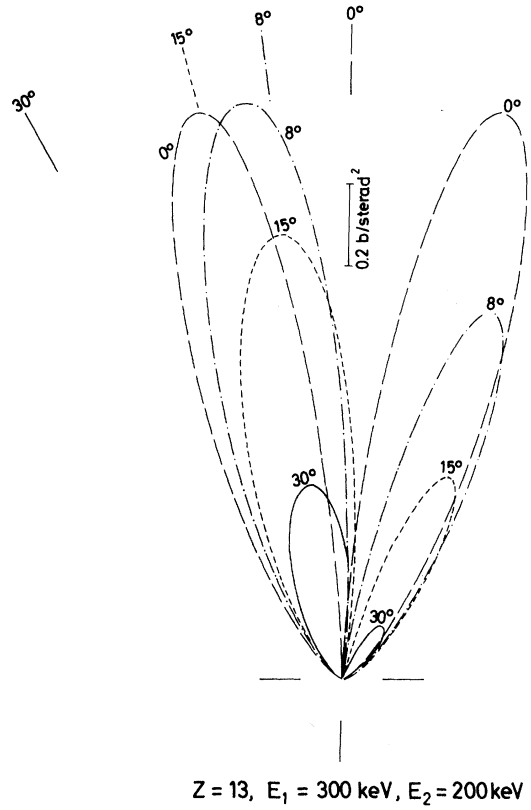

FIG. 8. Photon distributions computed from formula (30) for various electron angles θ_e.

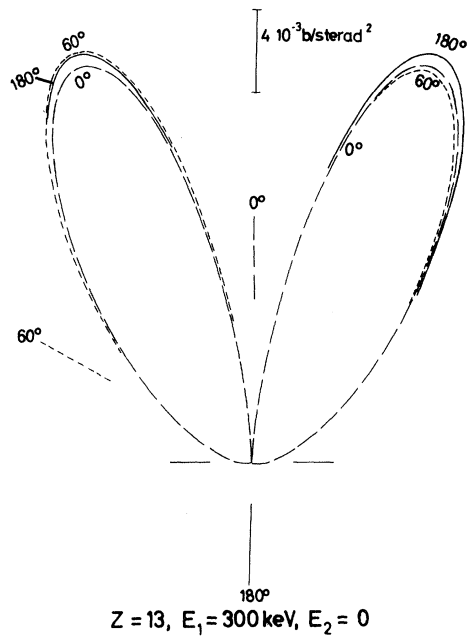

FIG. 10. Theoretical photon distributions at the short-wavelength limit for various electron angles θ_e.

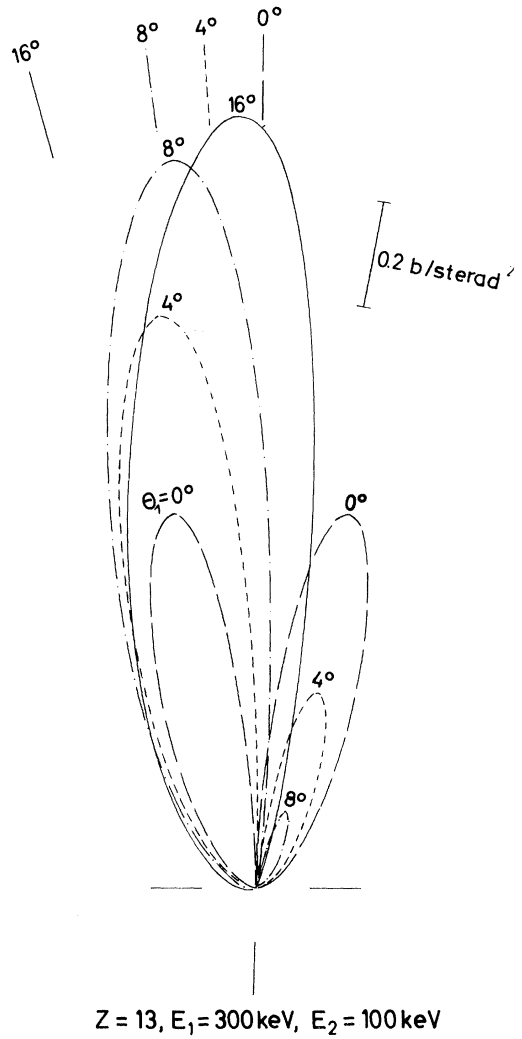

FIG. 9. Electron distributions computed from formula (30) for various photon angles θ_1.

10. INTEGRATED CROSS SECTION $d\sigma$

Integrating the cross section $d^2\sigma$ over the direction of emission of the photon, one obtains the cross section

$$\frac{d\sigma}{dk} = \int \frac{d^2\sigma}{dk d\Omega_k} d\Omega_k, \tag{62}$$

which is differential with respect to k only. It is drawn and compared with experimental values in Figs. 17(a) to 17(d) for $Z = 13$ and 79, $E_1 = 45$ and 500 keV. The agreement with the experiments of Motz and Placious[19,23] is fairly good for small energies and for large as well as for small Z. At $E_1 = 500$ keV, the agreement is, on the other hand, satisfactory only for $Z = 13$, whereas for $Z = 79$ the calculated cross section is less than

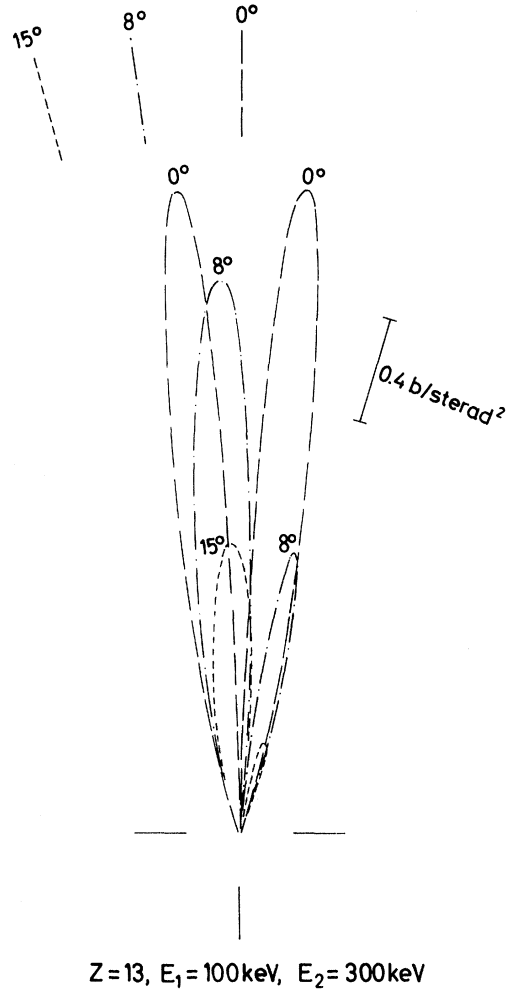

FIG. 11. Photon distributions computed from formula (30) for various electron angles θ_e.

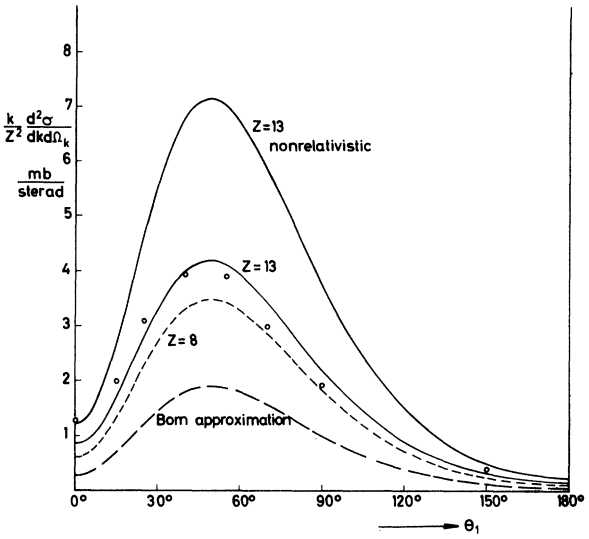

FIG. 12. Integrated photon distributions $d^2\sigma$ [calculated from formulas (58) and (30)] compared with experimental values, with nonrelativistic and Born-approximation cross section for $E_1 = 45$ keV, $E_2 = 5$ keV, $Z = 8$, and $Z = 13$.

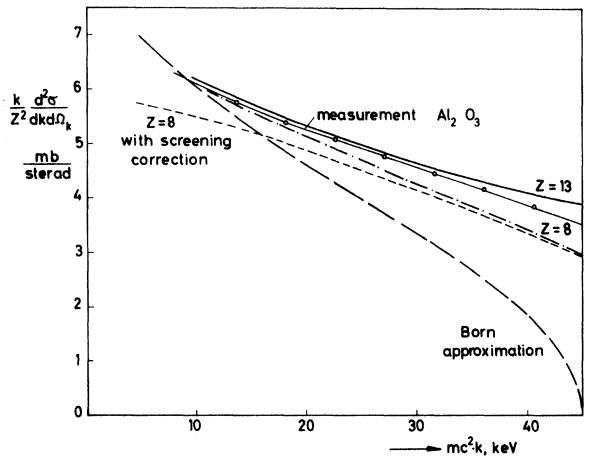

FIG. 13. Calculated x-ray spectra for $E_1 = 45$ keV, $Z = 8$ and $Z = 13$, and the photon angle $\theta_1 = 55^0$, compared with measurements at Al_2O_3 and Born-approximation cross sections.

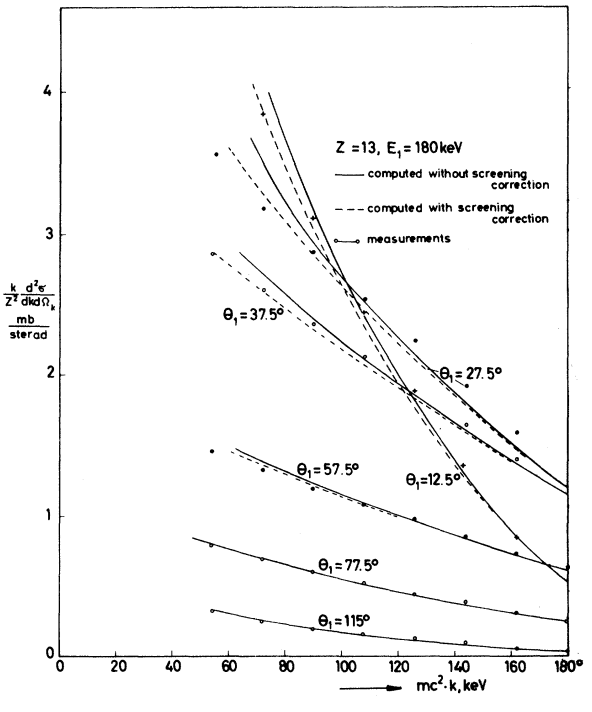

FIG. 14. X-ray spectra for $Z = 13$, $E_1 = 180$ keV for various photon angles θ_1, compared with experimental values.

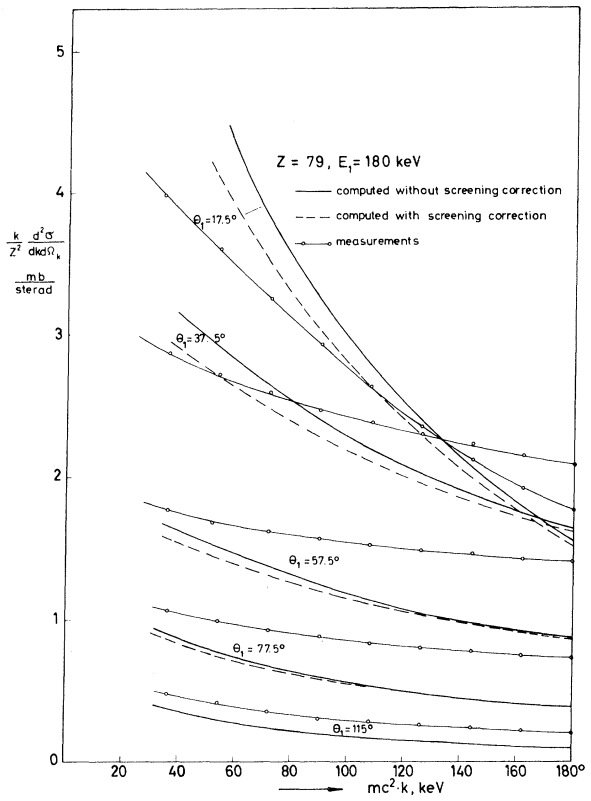

FIG. 15. X-ray spectra for $Z=79$, $E_1=180$ keV for various photon angles θ_1, compared with experimental values.

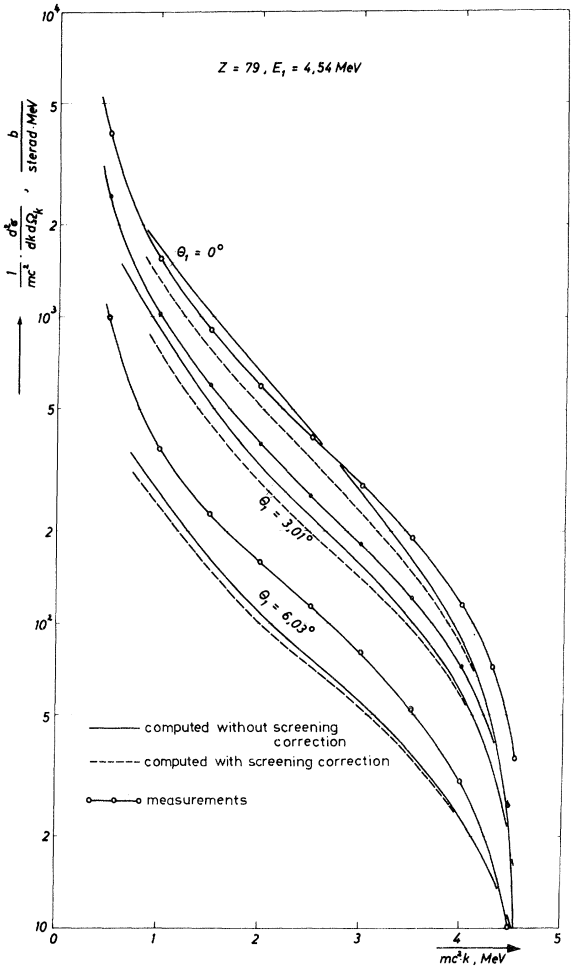

FIG. 16. X-ray spectra for $Z=79$, $E_1=4.54$ MeV for various photon angles θ_1, compared with experimental values.

the measured one by a factor of 2 nearly. It is to be noted, however, that experiments of Rester and Dance[20] result in cross sections $d\sigma$ which are considerably smaller than those of Motz at energies of the same order of magnitude (1 to 2.5 MeV). Besides the cross sections calculated with Sommerfeld-Maue eigenfunctions, we have also drawn the cross sections obtained by multiplying those of Bethe and Heitler by the factor (63) (cf. Sec. 11). Both these theoretical curves largely agree with one another; for $Z=13$ they even coincide within the degree of accuracy of our drawing.

Most of the authors dealing with bremsstrahlung at the short-wavelength limit have considered the cross section integrated over the angles of final electrons and photons, $d\sigma_0/dk$.[24–26] If Eq. (47) is integrated numerically over the solid angles $d\Omega p_2$ and $d\Omega_k$, the results are in good agreement with theoretical predictions and experimental values for low atomic numbers Z (cf. Table I). For high nuclear charges the agreement seems to be satisfactory if $k \lesssim \frac{1}{2}$. The asymptotic cross section for very high electron energies ϵ_1, $kd\sigma_0/dk$, is given by Eq. (47) with an accuracy of $\pm 5\%$ up to $Z \approx 47$ (Table II). It is too small by about 33% for $Z=79$ as compared with the results of Jabbur and Pratt,[25] which one can assume to be the most exact asymptotic cross sections.

11. COULOMB CORRECTION

The Born-approximation cross section becomes wrong in the short-wavelength limit (it goes to zero!) because the field of the nucleus strongly distorts the low-energy wave function from that of a plane wave. The cross section remains finite, however, if multiplied by an appropriate Coulomb correction factor. A factor of this kind has been derived for nonrelativistic energies using the formula for the total cross section $d\sigma$ calculated by Sommerfeld and Maue[27] with the exact Coulomb eigenfunctions neglecting retardation. Starting from the neighborhood of the long-wavelength limit, Elwert[4] has given the following correction factor

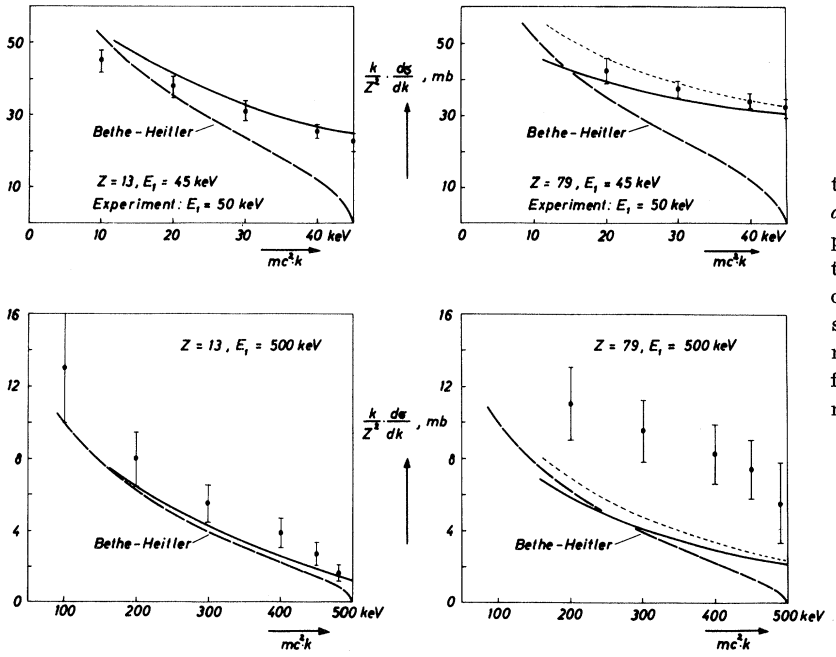

FIG. 17(a)–(d) Dependence of the bremsstrahlung cross section $d\sigma$ integrated over electron and photon angles on the photon energy; the solid curves, calculations; long-dashed curves, Born approximation; short-dashed curves, Born-approximation cross section multiplied by factor (63); and solid dots, measurement.

$$F_E = (a_2/a_1)(1 - e^{-2\pi a_1})/(1 - e^{-2\pi a_2}). \quad (63)$$

It agrees very closely up to terms of fourth order in a_1 with the correction factor for the short-wavelength limit. By analytical integration of the nonrelativistic expression (43) for $d^3\sigma$ over the directions of the final electrons, it has been shown that the factor (63) is independent of the direction of the outgoing photon in the neighborhood of the long-wavelength limit. As a_1 becomes smaller this range of constancy will become more and more extended towards the short-wavelength limit.[4]

Our present calculations make it possible to derive new numerically computed correction factors $F(\theta_1)$. They are given in Figs. 18 to 21 as functions of θ_1 for the same parameters as in Figs. 17(a) to 17(d). In addition the correction factor F_E is indicated by a mark on the ordinate.

TABLE I. Bremsstrahlung cross sections at the short-wavelength limit.

		$(k/Z^2)\, d\sigma_0/dk$ (mb)		
$h\nu = mc^2k$	Z	Eq. (47)	Fano *et al.* (Ref. 24)	Experimental values (Ref. 24) (extrapolated)
50 keV	13	22.1	21	21 ± 2
50 keV	79	27.0	23	31 ± 3
500 keV	13	1.17	1.3	1.5 ± 0.6
500 keV	79	2.09	3.4	5.2 ± 2.0
1 MeV	13	0.70	0.71	0.6 ± 0.3
1 MeV	79	1.29	1.8	1.7 ± 0.7
15 MeV	13	0.52	0.55	
15 MeV	79	0.88	1.77	1.47 ± 0.44

TABLE II. Theoretical asymptotic bremsstrahlung cross sections at the short-wavelength limit.

		$(k/Z^2)\, d\sigma_0/dk$ (mb)	
Z	Eq. (47)	Jabbur and Pratt (Ref. 25)	Deck *et al.* (Ref. 26)
13	0.52	0.493	0.493
47	0.92	0.971	0.943
79	0.86	1.286	1.164

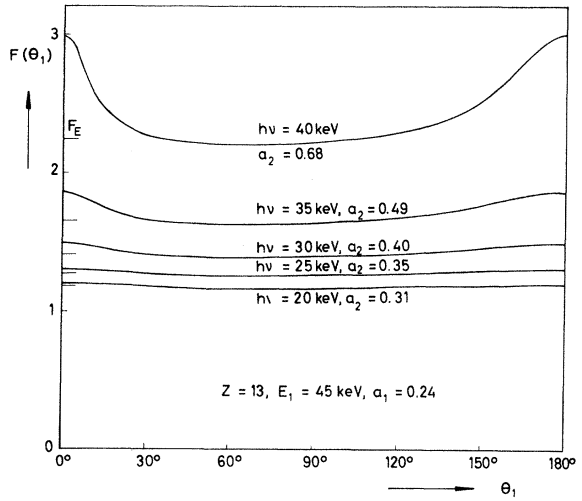

FIG. 18. Coulomb-correction factors $F(\theta_1)$. The factor F_E is indicated by marks on the ordinate.

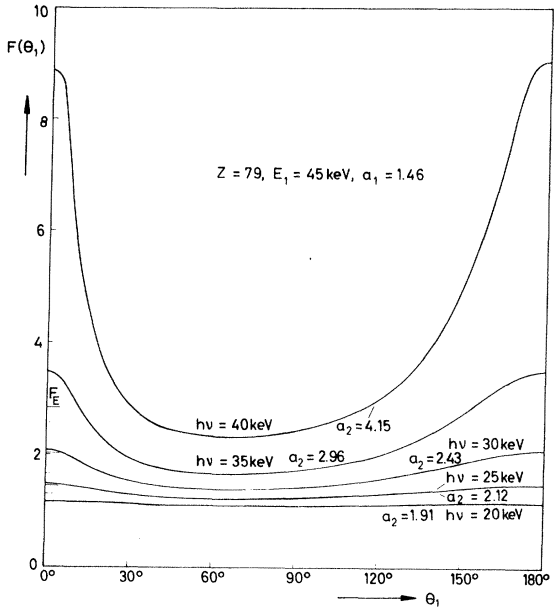

FIG. 19. Coulomb-correction factors $F(\theta_1)$. The factor F_E is indicated by marks on the ordinate.

In the neighborhood of the long-wavelength limit ($a_1 \approx a_2$) the functions $F(\theta_1)$ are indeed almost constant even for $a_1 > 1$. For small Z they have the value F_E for relativistic energies too. Approaching the short-wavelength limit, that is for increasing a_2, the constancy of $F(\theta_1)$ and the agreement with F_E remains for those angles, at which the main radiation is emitted, supposing that $a_1 \ll 1$; for $\theta_1 \to 0$ and $\theta_1 \to \pi$ the function $F(\theta_1)$ increases, especially if a_1 is not much smaller than unity. This amounts to a "filling up" of the minima of the cross section $d^2\sigma_B$ at forward and backward directions. The correction factor $F(\theta_1)$ has been measured by Klasmeier,[18] and he indeed finds such a "filling up" of the minima at the angles mentioned.

The Coulomb correction factor for the cross section $d\sigma_B$ integrated over the directions of outgoing electrons and photons agrees very well with F_E at low atomic numbers for both electron energies considered.

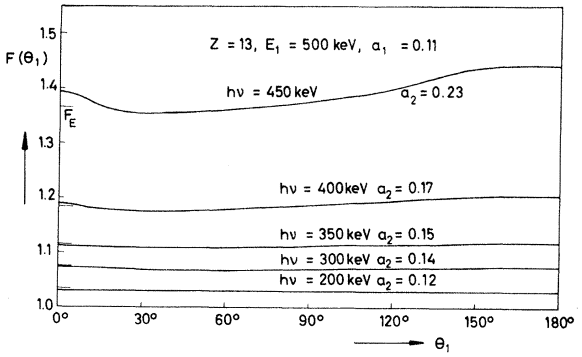

FIG. 20. Coulomb-correction factors $F(\theta_1)$. The factor F_E is indicated by marks on the ordinate.

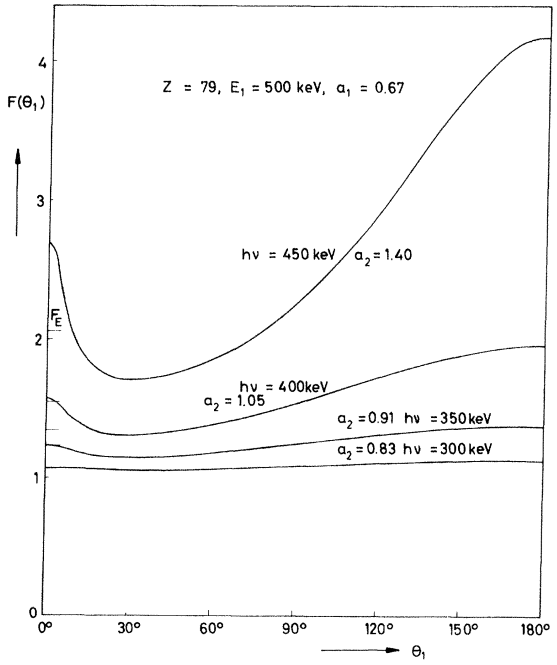

FIG. 21. Coulomb-correction factors $F(\theta_1)$. The factor F_E is indicated by marks on the ordinate.

ACKNOWLEDGMENTS

The authors are indebted to the Deutsche Forschungsgemeinschaft and the Bundesministerium für wissenschaftliche Forschung for financial grants. We wish to thank the Rechenzentrum of the University of Tübingen for providing calculation time.

[1]A. Sommerfeld, Ann. Physik 11, 257 (1931).
[2]C. G. Darwin, Proc. Roy. Soc. (London), Ser. A 118, 654 (1928).
[3]A. Sommerfeld and A. W. Maue, Ann. Physik 22, 629 (1935).
[4]G. Elwert, dissertation, University of Munich, W. Germany, 1939, published in part in Ann. Physik 34, 178 (1939); and in A. Sommerfeld, Atombau und Spektrallinien (Vieweg und Sohn, Braunschweig, Germany, 1951), Vol. II.
[5]F. Sauter, Ann. Physik 20, 404 (1934).
[6]H. Bethe and W. Heitler, Proc. Roy. Soc. (London), Ser. A 146, 83 (1934).
[7]O. Scherzer, Ann. Physik 13, 137 (1932).
[8]H. W. Furry, Phys. Rev. 81, 115 (1951).
[9]H. A. Bethe and L. C. Maximon, Phys. Rev. 93, 768 (1954).
[10]H. A. Bethe, L. C. Maximon, and F. Low, Phys. Rev. 91, 417 (1953).
[11]At the short-wavelength limit this has been checked with the aid of the modified Sommerfeld-Maue wave function of W. R. Johnson and C. J. Mullin, Phys. Rev. 119, 1270 (1960).
[12]A. T. Nordsieck, Phys. Rev. 93, 785 (1954).
[13]W. Nakel, Phys. Letters 22, 614 (1966); 25A, 569 (1967).
[14]W. Nakel, Z. Physik 214, 168 (1968).
[15]R. Hub and W. Nakel, Phys. Letters 24A, 601 (1967).
[16]E. Haug, dissertation, University of Tübingen, W. Germany, 1966 (unpublished).
[17]D. Roess, dissertation, University of Würzburg, W. Germany, 1959 (unpublished).
[18]G. Klasmeier, dissertation, University of Würzburg, W. Germany, 1962 (unpublished).
[19]J. W. Motz, Phys. Rev. 100, 1560 (1955).
[20]D. H. Rester and W. E. Dance, Phys. Rev. 161, 85 (1967).
[21]N. Starfelt and H. W. Koch, Phys. Rev. 102, 1598 (1956).
[22]G. Molière, Z. Naturforsch. 2a, 133 (1947).
[23]J. W. Motz and R. C. Placious, Phys. Rev. 109, 235 (1958).
[24]U. Fano, H. W. Koch, and J. W. Motz, Phys. Rev. 112, 1679 (1958).
[25]R. J. Jabbur and R. H. Pratt, Phys. Rev. 129, 184 (1963); 133, B1090 (1964).
[26]R. T. Deck, C. J. Mullin, and C. L. Hammer, Nuovo Cimento 32, 180 (1964).
[27]A. Sommerfeld and A. W. Maue, Ann. Physik 23, 589 (1935).